THE JOURNAL OF PHYSICAL CHEMISTRY A

Article

pubs.acs.org/JPCA

# Effect of Substituents on the Preferred Modes of One-Electron Reductive Cleavage of N−Cl and N−Br Bonds

Robert J. O'Reilly,*[†,‡] Amir Karton,[†] and Leo Radom*[†]

[†]School of Chemistry and ARC Centre of Excellence for Free Radical Chemistry and Biotechnology, University of Sydney, Sydney, NSW 2006, Australia

[‡]School of Chemistry, University of Tasmania, Private Bag 75, Hobart, TAS 7001, Australia

Supporting Information

**ABSTRACT:** In this study, we investigate the effect of substituents in determining the modes of one-electron reductive cleavage of X−NRR′ (X = Cl and Br) molecules. We achieve this through comparison of the calculated gas-phase electron affinities (EAs) and aqueous-phase one-electron reduction potentials ($E°$'s) for a range of nitrogen-centered radicals ($^{\bullet}$NRR′) with the corresponding EA and $E°$ values for $^{\bullet}$Cl and $^{\bullet}$Br. The gas-phase EAs have been obtained using the benchmark-quality W1w thermochemical protocol, whereas $E°$ values have been obtained by additionally applying free energy of solvation corrections, obtained using the conductor-like polarizable continuum (CPCM) model. We find that the N-halogenated derivatives of amines and amides should generally cleave in such a way as to afford $^{\bullet}$NRR′ and $X^{-}$. For the N-halogenated imides, on the other hand, the N-brominated derivatives are predicted to produce $^{\bullet}$Br in solution, whereas the N-chlorinated derivatives again would give $Cl^{-}$. Importantly, we predict that *N*-bromouracil is likely to afford $^{\bullet}$Br. This may have important implications in terms of inflammatory-related diseases, because $^{\bullet}$Br may damage biomolecules such as proteins and DNA. To assist in the determination of the gas-phase EAs of larger $^{\bullet}$NRR′ radicals, not amenable to investigation using W1w, we have evaluated the performance of a wide range of lower-cost theoretical methods. Of the standard density functional theory (DFT) procedures, M06-2X, $\tau$-HCTHh, and B3-LYP show good performance, with mean absolute deviations (MADs) from W1w of 4.8−6.8 kJ mol$^{-1}$, whereas ROB2-PLYP and B2-PLYP emerge as the best of the double-hybrid DFTs (DHDFTs), with MADs of 2.5 and 3.0 kJ mol$^{-1}$, respectively. Of the G*n*-type procedures, G3X and G4 show very good performance (MADs = 2.4 and 2.6 kJ mol$^{-1}$, respectively). The G4(MP2)-6X+ procedure performs comparably, with an MAD of 2.7 kJ mol$^{-1}$, with the added advantage of significantly reduced computational expense.

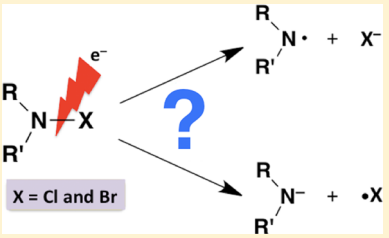


## 1. INTRODUCTION

During the inflammatory response, the enzymes myeloperoxidase and eosinophil peroxidase catalyze the oxidation of $Cl^{-}$ and $Br^{-}$ (by $H_2O_2$), affording hypochlorous (HOCl) and hypobromous (HOBr) acids, respectively. These are potent oxidants that serve an important role in the host defense mechanism, largely because they act in such a way as to incapacitate invading pathogens (e.g., bacteria, viruses, and fungi).[1] These oxidants may react with a wide range of functional groups, but increasing attention has been given to their reaction with nitrogen-containing functionalities, as these are found in great abundance in biological systems (for example, proteins are made up of peptide linkages, whereas the DNA/RNA bases also contain reactive nitrogen-containing groups).[2] The resulting products of such reactions are N-halogenated derivatives of amines, amides, imides, or imines.

Because of the substantially weaker nature of N−X (X = Cl and Br) vs N−H bonds, N-halogenated species are more susceptible to radical formation via N−X bond homolysis. Given that radical formation is likely to be important from the perspective of disease, we have previously studied the effect of substituents on the strength of N−X bonds with regard to spontaneous homolytic cleavage.[3] Although thermally induced cleavage processes are relatively slow, the addition of one-electron donors, such as transition metal ions (e.g., $Cu^{+}$ and $Fe^{2+}$), superoxide ($O_2^{\bullet -}$), or hydrated electrons ($e^{-}_{aq}$), expedites the dissociation process.[4,5] The addition of a single electron to the N−X-containing species affords the possibility of two different sets of products. Thus, dissociative one-electron reduction of the N−X bonds of N-halogenated species may lead to expulsion of either a halide anion ($X^{-}$) plus a nitrogen-centered radical ($^{\bullet}$NRR′)

$$X{-}NRR' + e^{-} \rightarrow X^{-} + {}^{\bullet}NRR' \quad (1)$$

or a halogen atom ($^{\bullet}$X) plus a nitrogen-centered anion ($^{-}$NRR′):

$$X{-}NRR' + e^{-} \rightarrow {}^{\bullet}X + {}^{-}NRR' \quad (2)$$

On the basis of available experimental studies, when X = Cl, cleavage appears to follow eq 1, irrespective of the substituents (i.e., R/R′) bound to the nitrogen.[4] When X = Br, cleavage is generally consistent with eq 1, except for the specific case of *N*-

**Received:** October 10, 2012
**Revised:** December 12, 2012
**Published:** January 3, 2013

   dx.doi.org/10.1021/jp310048f | *J. Phys. Chem. A* 2013, 117, 460−472

bromoimides, where it is found experimentally that some species (e.g., the N-brominated derivatives of succinimide and glutarimide) undergo cleavage that results in the expulsion of $^{\bullet}$Br (i.e., via eq 2).[5] From a biological perspective, the formation of $^{\bullet}$Br in vivo is expected to be deleterious to host tissues. First, $^{\bullet}$Br is known to participate in hydrogen-atom-abstraction reactions from the backbone $\alpha$-C−H moieties of amino acids (and hence provides a route to protein degradation).[6] Second, the reaction of $^{\bullet}$Br with excess $Br^-$ affords $Br_2^{\bullet-}$, a powerful oxidant ($E^\circ$ = +1.66 V),[7] which has been shown to oxidize free nucleobases[8] as well as those in plasmid DNA.[9]

From a thermodynamic viewpoint, the products arising from one-electron reduction of N−X-containing species in the gas phase may be determined by comparing the electron affinities (EAs) of the nitrogen-centered radical ($^{\bullet}$NRR′) and $^{\bullet}$X. The EAs of $^{\bullet}$NRR′ and $^{\bullet}$X (X = Cl/Br) may be written in terms of eqs 3 and 4, respectively, and correspond to the energy liberated when an electron is added to a neutral species.

$$^{\bullet}\mathrm{NRR'} + e^- \rightarrow {}^-\mathrm{NRR'} \quad (3)$$

$$^{\bullet}\mathrm{X} + e^- \rightarrow \mathrm{X}^- \quad (4)$$

By convention, a positive EA corresponds to a situation in which the electron is bound to the neutral $^{\bullet}$NRR′ or $^{\bullet}$X radicals; i.e., the EAs are the negative of the energy changes in reactions 3 and 4. If EA($^{\bullet}$X) < EA($^{\bullet}$NRR′), then the greater propensity for an electron to bind to $^{\bullet}$NRR′, rather than to $^{\bullet}$X would result in the one-electron reduction of XNRR′ giving $^{\bullet}$X plus $^-$NRR′.

In aqueous solution, the corresponding quantities of interest are the one-electron reduction potentials ($E^\circ$). The more positive the value of $E^\circ$, the more favorable is the binding of the electron. Thus, if $E^\circ$($^{\bullet}$X/X$^-$) < $E^\circ$($^{\bullet}$NRR′/$^-$NRR′), then the products of the dissociative one-electron reduction of X−NRR′ are expected to be $^{\bullet}$X plus $^-$NRR′.

We have used this approach previously[5a] to examine the preferred mode of cleavage of a small number of N-halogenated species, by comparing the EAs and $E^\circ$ values for the associated radicals (namely $^{\bullet}NH_2$, $^{\bullet}NHCH_3$, $^{\bullet}NHCF_3$, imidazolyl, $^{\bullet}$NHCHO, $^{\bullet}N(CHO)_2$, and succinimidyl) with those of $^{\bullet}$Cl and $^{\bullet}$Br, where we obtained the EAs using the high-level G4 theoretical procedure.[5a] The present paper extends our previous investigation by substantially increasing the number of systems investigated (from 7 systems to 31), and using a higher level of theory (namely the nonempirical W1w thermochemical protocol[10] in place of G4) for obtaining the underlying gas-phase EAs. We address a question that is of particular importance to biological systems, namely whether the *N*-chloro or *N*-bromo derivatives of uracil are likely to provide a source of $^{\bullet}$X in vivo. Finally, we assess the performance of a range of lower-cost theoretical procedures, including standard density functional theory (DFT) procedures, more recent double-hybrid DFT (DHDFT) methods, and composite G*n* thermochemical protocols relative to benchmark W1w reference values for the calculation of the EAs of $^{\bullet}$NRR′ radicals.

## 2. COMPUTATIONAL PROCEDURES

All structures were obtained at the B3-LYP/A′VTZ level of theory, where A′V*n*Z indicates the combination of the standard cc-pV*n*Z basis sets[11a] on H, aug-cc-pV*n*Z basis sets[11b] on first-row atoms and Br, and aug-cc-pV(*n*+d)Z basis sets[11c] on Cl. Harmonic vibrational frequencies have been calculated at the same level of theory to confirm that the stationary points are equilibrium structures; i.e., they have only real frequencies. These frequencies were also used to calculate zero-point vibrational energy (ZPVE), and thermal enthalpy ($H$) and entropy ($S$) corrections. The contributions were scaled according to factors reported in the literature (specifically, 0.9884 for ZPVE, 0.9987 for $H$, and 1.0043 for $S$).[12] Higher-level W1w calculations have been performed on these structures to obtain accurate adiabatic gas-phase EAs for all species. W1w theory represents a layered extrapolation to the all-electron, relativistic CCSD(T) complete-basis-set limit, and has been explained in detail elsewhere.[10] It differs from the older W1 procedure through the use of aug′-cc-pV(*n*+d)Z basis sets, rather than aug′-cc-pV(*n*+2d1f)Z basis sets for the extrapolations of the Hartree−Fock, valence CCSD and (T) components.[10a] In brief, the Hartree−Fock (ROHF) energy is extrapolated from the A′VTZ and A′VQZ basis sets using the two-point extrapolation formula $E(L) = E_\infty + A/L^\alpha$, where $L$ is the highest angular momentum present in the basis set and $\alpha$ = 5 is the extrapolation exponent. The valence ROCCSD correlation energy is extrapolated from the same basis sets using the above two-point extrapolation formula with $\alpha$ = 3.22. The valence parenthetical triples (T) correlation component is extrapolated from the A′VDZ and A′VTZ basis sets using the same two-point extrapolation formula. The inner-shell correlation contribution is obtained at the ROCCSD(T) level in conjunction with the MTsmall core-correlation basis set (where MTsmall denotes a completely uncontracted cc-pVTZ basis set with additional 2d1f high-exponent functions).[10a] The deep-core orbitals (i.e., the 1s orbital for chlorine, and the 1s, 2s, and 2p orbitals for bromine) have been constrained to be doubly occupied in all configurations. This choice of deep-core-valence partitioning has been justified previously.[10] The scalar-relativistic contribution is obtained from second-order Douglas−Kroll−Hess[13] CCSD(T)/MTsmall calculations (within the frozen-core approximation). In obtaining the energies of the halogen atoms, spin−orbit corrections of 3.52 (for Cl$^{\bullet}$) and 14.69 (for Br$^{\bullet}$) kJ mol$^{-1}$ have been applied.[14]

For the calculation of reduction potentials in aqueous solution, the effect of bulk water was estimated through the calculation of free energies of solvation ($\Delta G_{solv}$) at the HF/6-31+G(d) level in conjunction with the conductor-like polarizable continuum model (CPCM) with Bondi radii.[15] This approach has been shown to provide $\Delta G_{solv}$ energies with a mean absolute deviation from experimental values of 15.2 kJ mol$^{-1}$ for a test set of 70 species including neutrals, cations, and anions.[16] Combination of $\Delta G_{(gas)}$ and $\Delta G_{solv}$ yields $\Delta G_{(aq)}$ values that correspond to 298 K and 1 M (Figure 1). Furthermore, as the electron-addition reaction does not involve changes in the number of molecules, no change-of-state correction is required to account for the change from the gas phase (1 atm) to solution (1 M).

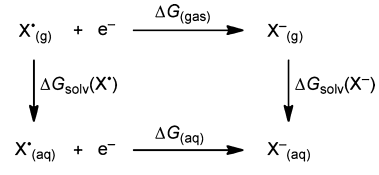


**Figure 1.** Thermodynamic cycle by which $\Delta G_{(aq)}$ values are computed.


dx.doi.org/10.1021/jp310048f | J. Phys. Chem. A 2013, 117, 460−472

Absolute reduction potentials have then been calculated from $\Delta G_{(aq)}$, and these are converted to reduction potentials ($E°$) relative to the standard hydrogen electrode (SHE). This involves subtracting the estimated absolute reduction potential of 4.43 V for hydrogen[17] from the absolute reduction potentials of the radicals (note that $n$ refers to the number of electrons involved in the reduction and $F$ is the Faraday constant):

$$E° = (-\Delta G_{(aq)}/nF) - 4.43\ \text{V} \quad (5)$$

To facilitate future investigations of the EAs of larger •NRR′ systems, for which the W1w procedure may not be feasible, the performance of a range of lower-cost theoretical procedures has been assessed, namely standard DFT procedures, double-hybrid DFT (DHDFT) procedures, and a number of Gaussian-$n$ (G$n$) thermochemical protocols.

The standard DFT exchange−correlation functionals considered in the present study (ordered by their rung on Jacob's ladder[18]) are the local density approximation (LDA) SVWN5;[19] variants of the pure generalized gradient approximation (GGA) (B-LYP,[20,21] B-P86,[20,22] PBE,[23] HCTH407,[24] and B97-D);[25] the meta-GGAs (MGGAs) (VSXC,[26] TPSS,[27] $\tau$-HCTH,[28] and M06-L);[29] the hybrid-GGAs (HGGAs) (PBE0,[30] B3-PW91,[31,32] B3-P86,[22,31] B97-1,[33] B98,[34] TPSSh,[35] B3-LYP,[31,21,36] X3-LYP,[37] BH&HLYP,[38] $\omega$B97,[39] $\omega$B97X,[39] and $\omega$B97X-D);[40] and the hybrid-meta-GGAs (HMGGAs) (B1-B95,[20,41] BMK,[42] $\tau$-HCTHh,[28] M05,[43] M05-2X,[44] M06,[45] M06-2X,[45] and M06-HF).[45] The sensitivity of the performance of the standard DFT procedures with respect to choice of basis set was also investigated and was carried out in conjunction with the following basis sets: (i) the 6-31+G(d,p), 6-31+G(2df,p), and 6-311+G(3df,2p) basis sets of Pople and co-workers and (ii) the A′V$n$Z ($n$ = D, T, Q) correlation-consistent basis sets of Dunning and co-workers.[11] The double-hybrid DFT procedures investigated include B2-PLYP,[46] B2K-PLYP,[47] B2GP-PLYP,[48] and ROB2-PLYP.[49] The performance of these procedures has been assessed, within the frozen-core approximation, in conjunction with the A′V$n$Z ($n$ = D, T, Q) basis sets. The DuT and PoT procedures,[50] which were parametrized specifically for use in conjunction with triple-$\zeta$-quality basis sets, have also been assessed.

In addition, the performance of the composite thermochemical G$n$ procedures G3X,[51] G3X(MP2),[52] G3X(MP2)-RAD,[53] G4,[54] G4-5H,[55] G4(MP2),[56] G4(MP2)-6X,[57] and G4(MP2)-6X+[58] was also assessed. We note that the geometries used for the DFT and G$n$ calculations are the same as those employed for the W1w reference energies (i.e., optimized at the B3-LYP/A′VTZ level of theory).

All geometry optimizations, standard and double-hybrid DFT calculations, and calculations required to compute G$n$ energies were performed using Gaussian 09.[59] The free energy of solvation corrections ($\Delta G_{solv}$) necessary for the calculation of $E°$ values were obtained using Gaussian 03,[60] to maintain the same implementation of CPCM as employed in the benchmark solvation study.[16] The Hartree−Fock and CCSD(T) calculations necessary to compute W1w energies were performed using Molpro 2009.1.[61]

## 3. RESULTS AND DISCUSSION

**3.1. Performance of the W1w Procedure for the Calculation of Gas-Phase Adiabatic EAs.** It has generally been found that the W1 procedure shows good performance for the calculation of electron affinities. For example, for the 25 EAs of small molecules in the G2-1 test set,[62] W1 attains a mean absolute deviation (MAD) from experimental values of 1.5 kJ mol$^{-1}$.[10c] For the set of 32 EAs of larger systems found in the G2-2 test set,[63] W1 affords an MAD of 1.8 kJ mol$^{-1}$.[10c] These MADs imply a 95% confidence interval of about 5.0 kJ mol$^{-1}$ for the W1 procedure. It should be mentioned that for other thermochemical properties (such as reaction energies, bond dissociation energies, and enthalpies of formation) W1 performs equally well.[10] For example, for a set of 124 highly accurate total atomization energies covering a broad spectrum of bonding situations, W1 attains an MAD of just 2.0 kJ mol$^{-1}$.[10f]

The EAs of a small number of radicals relevant to the cleavage of N−X bonds (X = Cl and Br) have been determined experimentally.[64] Table 1 compares our W1w EAs with the experimental ones, and lists the mean absolute deviation (MAD), mean deviation (MD), and largest deviations (LDs) of W1w from experimental values. In general, the W1w procedure exhibits reasonably good to excellent performance relative to experiment, with an MAD and MD of 2.9 kJ and 1.1 kJ mol$^{-1}$, respectively. In all but one case (the 1,2,3-triazolyl radical), our W1w EAs agree with experiment to within overlapping uncertainties. For the 1,2,3-triazolyl radical, a deviation of +7.2 kJ mol$^{-1}$ is obtained (Table 1). For the two halogens, namely •Cl and •Br, the deviations are 1.4 and 1.9 kJ mol$^{-1}$, respectively.

**Table 1. Performance of the W1w Procedure for the Calculation of Adiabatic Gas-Phase Electron Affinities (EAs) of Radicals Resulting from Cleavage of N−X Bonds (X = Cl and Br) (298 K, kJ mol$^{-1}$)**

| radical | W1w | expt |
|---|---|---|
| •$NH_2$ | 72.1 | 74.4 ± 0.5[a] |
| •$NHCH_3$ | 44.5 | 41.7 ± 1.4[b] |
| •$N(CH_3)_2$ | 52.4 | 48.6 ± 2.9[b] |
| •NHPh | 157.2 | 164.4 ± 2.9[c] |
| •imidazolyl | 252.9 | 252.1 ± 0.6[d] |
| •pyrrolyl | 208.5 | 207.0 ± 1.0[e] |
| •pyrazolyl | 285.8 | 283.5 ± 0.5[f] |
| •1,2,3-triazolyl | 339.8 | 332.6 ± 0.4[g] |
| •N=$CH_2$ | 49.1 | 49.3 ± 0.8[h] |
| •Cl | 350.1 | 348.7 ± 0.0[i] |
| •Br | 326.4 | 324.5 ± 0.0[j] |
| MAD | 2.9 | |
| MD | +1.1 | |
| LD | −7.2, +7.2 | |

[a]Reference 64a. [b]Reference 64b. [c]Reference 64c. [d]Reference 64d. [e]Reference 64e. [f]Reference 64f. [g]Reference 64g. [h]Reference 64h. [i]Reference 64i. [j]Reference 64j.

Because W1w represents a layered extrapolation to the all-electron CCSD(T) basis-set-limit energy, it is of interest to estimate whether the contributions from post-CCSD(T) excitations are likely to be significant for the species considered in the present work. The percentage of the atomization energy accounted for by parenthetical connected triple excitations, % $TAE_e$[(T)], has been shown to be a reliable energy-based diagnostic that provides an indication of the importance of post-CCSD(T) contributions.[10e] Table S1 of the Supporting Information gathers the % $TAE_e$[(T)] values for the radicals and anions considered in the present study, and they can be


dx.doi.org/10.1021/jp310048f | J. Phys. Chem. A 2013, 117, 460−472

seen generally to lie in the range 1.3−3.3%. The largest values occur for the tetrazolyl radical and anion (5.4 and 4.7%, respectively), $F_2C{=}N^-$ (4.1%), and the anions and radicals associated with the 1,2,3- and 1,2,4-triazoles (3.6−3.9%). On the basis of the above results, the use of the W1w procedure for investigating the EAs of the radicals relevant to N−X bond cleavage (X = Cl and Br) appears to be warranted.

**3.2. Definitions Relating to the Relative Stabilities of Radicals and Anions, and the Relation of Such Quantities to the EAs.** To facilitate an analysis of the effect of substituents on the relative magnitudes of the EAs (compared with that for $^\bullet NH_2$), it is necessary to consider the effects in both the radical *and* the anion. To do this, we will use the same approach that we used in our previous investigation.[5a] For the radicals, the effect of substituents on the relative stabilities has been considered through the calculation of widely used *radical stabilization energies* (RSEs). The RSE is defined as the energy change for the hydrogen-transfer reaction presented in eq 6:

$$\text{RSE:}\qquad {}^\bullet NRR' + H{-}NH_2 \rightarrow H{-}NRR' + {}^\bullet NH_2 \qquad (6)$$

The RSE measures the effect of the substituents (R and R′) on the stability of the radical ($^\bullet$NRR′) relative to their effect in the closed-shell molecule HNRR′. A positive value indicates relative stabilization of the radical.

Similarly, the *anion stabilization energy* (ASE) is defined as the energy change for the proton-transfer reaction shown in eq 7:

$$\text{ASE:}\qquad {}^-NRR' + H{-}NH_2 \rightarrow H{-}NRR' + {}^-NH_2 \qquad (7)$$

The ASE measures the effect of the substituents (R and R′) on the stability of the anion ($^-$NRR′) relative to their effect in the neutral HNRR′ species. A positive value indicates relative stabilization of the anion.

Differences in the EA of a substituted radical $^\bullet$NRR′ from the EA of the parent radical $^\bullet NH_2$ (denoted $\Delta EA(^\bullet NRR')$) can be related to the effect of the substituents (R and R′) on the individual anion and radical according to eq 8:

$$\Delta EA({}^\bullet NRR') = ASE({}^-NRR') - RSE({}^\bullet NRR') \qquad (8)$$

**3.3. EA and $E°$ Data set for $^\bullet$NRR′ and $^\bullet$X (*X* = Cl and Br) Radicals.** Table 2 presents the EA, RSE, ASE, and $E°$ values for a number of radicals or anions relevant to the one-electron reductive cleavage of X−NRR′ (X = Cl and Br), which have been obtained at the W1w level (and the computationally more economical W1-F12 method[65] in the case of the 3-uracilyl radical). These thermochemical quantities are used in the following sections to provide insights into the factors affecting the preferred modes of cleavage of X−NRR′ molecules upon one-electron reduction in both the gas and aqueous phases. The discussion has been structured in such a way that we will first comment on the EA and $E°$ values of the various classes of radicals (i.e., aminyl, heterocyclic, amidyl, imidyl and iminyl). We will then proceed to discuss the preferred modes of cleavage of X−NRR′ molecules (X = Cl and Br) in broader terms by comparing the EA and $E°$ values of the nitrogen-centered radicals with those of $^\bullet$Cl and $^\bullet$Br.

*3.3.1. EA and $E°$ Values of Aminyl Radicals.* We have investigated the EAs of a number of aminyl-type radicals (Table 2). Compared with the EA of $^\bullet NH_2$ (72.1 kJ mol$^{-1}$), the introduction of one or two electron-donating methyl substituents (as in $^\bullet NHCH_3$ and $^\bullet N(CH_3)_2$) induces a lowering

**Table 2. Adiabatic Electron Affinities (EAs), Radical Stabilization Energies (RSEs), Anion Stabilization Energies (ASEs), Free Energy of Solvation Corrections ($\Delta\Delta G_{solv}$), and Aqueous One-Electron Reduction Potentials ($E°$ in Volts, Relative to SHE) for Radicals or Anions Relevant to Cleavage of N−X Bonds (X = Cl and Br) (298 K, kJ mol$^{-1}$)[a]**

| radical | EA | RSE | ASE | $\Delta\Delta G_{solv}$[b] | $E°$ |
|---|---|---|---|---|---|
| $^\bullet NHCH_3$ | 44.5 | 31.9 | 4.4 | −332.7 | −0.54 |
| $^\bullet N(CH_3)_2$ | 52.4 | 55.5 | 35.8 | −296.9 | −0.90 |
| $^\bullet NH_2$ | 72.1 | 0.0 | 0.0 | −361.3 | +0.04 |
| $^\bullet NHCH_2CO_2H$ | 105.8 | 26.4 | 60.1 | −288.2 | −0.38 |
| $^\bullet$NHPh | 157.2 | 65.9 | 151.1 | −248.9 | −0.23 |
| $^\bullet NHCF_3$ | 266.5 | −10.9 | 183.6 | −257.9 | +0.99 |
| $^\bullet$pyrrolyl | 208.5 | 50.0 | 186.4 | −247.5 | +0.27 |
| $^\bullet$imidazolyl | 252.9 | 45.2 | 226.0 | −239.0 | +0.64 |
| $^\bullet$pyrazolyl | 285.8 | −8.1 | 205.6 | −258.9 | +1.18 |
| $^\bullet$1,2,3-triazolyl | 339.8 | −9.7 | 258.0 | −232.7 | +1.45 |
| $^\bullet$1,2,4-triazolyl | 331.1 | −9.3 | 249.8 | −249.3 | +1.56 |
| $^\bullet$tetrazolyl | 401.7 | −21.0 | 308.6 | −244.1 | +2.22 |
| $^\bullet NHCHO$ | 280.7 | −29.3 | 179.3 | −303.3 | +1.48 |
| $^\bullet NHCOCH_3$ | 267.3 | −21.7 | 173.5 | −302.0 | +1.25 |
| $^\bullet NHCFO$ | 325.6 | −34.6 | 218.9 | −253.3 | +1.53 |
| $^\bullet NHCOCN$ | 384.1 | −38.8 | 273.2 | −239.3 | +1.91 |
| $^\bullet NHCONH_2$ | 250.5 | −7.9 | 170.5 | −288.6 | +0.94 |
| $^\bullet N(CH_3)CHO$ | 257.8 | −7.2 | 178.5 | −287.9 | +1.06 |
| $^\bullet NHCH{=}NH$ | 198.2 | 25.1 | 151.3 | −298.7 | +0.64 |
| $^\bullet NH(NH_2)C{=}NH$ | 204.2 | 25.3 | 157.5 | −298.8 | +0.66 |
| $^\bullet$glutarimidyl | 350.1 | −52.4 | 225.7 | −251.9 | +1.79 |
| $^\bullet N(CHO)_2$ | 390.5 | −52.0 | 266.4 | −226.0 | +1.96 |
| $^\bullet$succinimidyl | 395.9 | −69.6 | 254.3 | −243.4 | +2.11 |
| $^\bullet$3-uracilyl[c] | 379.0 | −67.1 | 240.8 | −248.4 | +2.04 |
| $^\bullet N{=}CH_2$ | 49.1 | 80.4 | 57.4 | −312.3 | −0.70 |
| $^\bullet N{=}C(CH_3)_2$ | 51.8 | 70.4 | 50.1 | −305.3 | −0.76 |
| $^\bullet N{=}CHCH_3$ | 61.1 | 72.1 | 61.2 | −307.3 | −0.63 |
| $^\bullet N{=}CH(NH_2)$ | 94.0 | 42.7 | 64.5 | −301.8 | −0.34 |
| $^\bullet N{=}C(NH_2)_2$ | 99.3 | 34.7 | 61.9 | −299.6 | −0.31 |
| $^\bullet N{=}CH(OH)$ | 148.0 | 30.4 | 106.3 | −311.6 | +0.10 |
| $^\bullet N{=}CF_2$ | 258.6 | 2.2 | 188.8 | −272.7 | +1.05 |
| $^\bullet$Cl | 350.1 | | | −309.3 | +2.39 |
| $^\bullet$Br | 326.4 | | | −276.9 | +1.80 |

[a]Obtained at the W1w level, unless otherwise noted. [b]$\Delta\Delta G_{solv} = \Delta G_{solv}(\text{anion}) - \Delta G_{solv}(\text{radical})$. [c]Obtained at the W1-F12 level.

in the EAs of the resulting radicals (EAs = 44.5 and 52.4 kJ mol$^{-1}$, respectively). However, the EAs do not vary in a monotonic fashion with the degree of methylation, viz., $EA(^\bullet NH_2) > EA(^\bullet N(CH_3)_2) > EA(^\bullet NHCH_3)$. The EA of $^\bullet N(CH_3)_2$ is larger than that of $^\bullet NHCH_3$, and this arises because of the particularly large ASE associated with $^-N(CH_3)_2$ (35.8 kJ mol$^{-1}$) vs that of $^-NHCH_3$ (4.4 kJ mol$^{-1}$), relative to the smaller RSE differential between $^\bullet N(CH_3)_2$ (55.5 kJ mol$^{-1}$) and $^\bullet NHCH_3$ (31.9 kJ mol$^{-1}$). The increased C−H bond lengths in $^-N(CH_3)_2$ (1.133 Å) compared with $^-NHCH_3$ (1.128 Å), which are indicative of a greater extent of donation of excess electron density into acceptor $\sigma^*_{C-H}$ orbitals in the former, are consistent with the larger ASE of $^-N(CH_3)_2$ (Figure 2). In support of this, natural bond orbital (NBO) calculations (at the B3-LYP/A′VTZ level) show that the stabilizing LP(N) → $\sigma^*_{C-H}$ interactions in $^-N(CH_3)_2$ are of


dx.doi.org/10.1021/jp310048f | J. Phys. Chem. A 2013, 117, 460−472

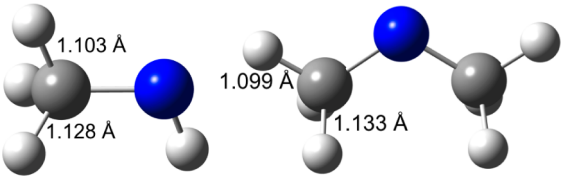


**Figure 2.** Geometries of the methyl- and dimethyl-substituted nitrogen-centered anions (which adopt $C_s$ and $C_{2v}$ symmetry, respectively).

greater magnitude than in $^{-}NHCH_3$ ($E_{(2)}$ ~ 52.0 vs 47.7 kJ mol$^{-1}$, respectively).

We have investigated the effect of the $\sigma$-electron-withdrawing sp$^3$-hybridized $CH_2CO_2H$ and $CF_3$ groups. Although attachment of the $CH_2CO_2H$ group (i.e., as in the nitrogen-centered isomer of the glycyl radical) induces a modest increase in the EA compared with that of $^{\bullet}NH_2$ (105.8 vs 72.1 kJ mol$^{-1}$), the EA of $^{\bullet}NHCF_3$ is substantially larger (266.5 kJ mol$^{-1}$). The particularly large EA of the latter is, for the most part, attributable to the existence of a large stabilizing effect in $^{-}NHCF_3$ (ASE = 183.6 kJ mol$^{-1}$), arising as a result of the donation of the excess electron density into electron-accepting $\sigma^*_{C-F}$ orbitals. We have also considered the effect of the $\pi$-accepting Ph substituent, computing an EA of 157.2 kJ mol$^{-1}$ for $^{\bullet}NHPh$. The substantially larger EA of $^{\bullet}NHCF_3$ vs $^{\bullet}NHPh$ arises partly because of a difference in the extent to which the anions are stabilized (ASEs = 183.6 vs 151.1 kJ mol$^{-1}$), but even more so because delocalization of the unpaired electron throughout the ring system in the $^{\bullet}NHPh$ radical leads to a stabilizing effect (RSE = 65.9 kJ mol$^{-1}$), whereas the $^{\bullet}NHCF_3$ radical is subject to a destabilizing effect (RSE = −10.9 kJ mol$^{-1}$).

We now examine the aqueous one-electron reduction potentials ($E°$) of the aminyl radicals. These species are generally predicted to be reducing agents; i.e., most of the $E°$ values are negative. The main exception to this is $^{\bullet}NHCF_3$ which, due to its particularly large underlying gas-phase EA, has an $E°$ value of +0.99 V. As a result, $^{\bullet}NHCF_3$ is predicted to exhibit the characteristics of a mild oxidant. It is also of interest to note that, whereas the gas-phase EA of $^{\bullet}NH_2$ is substantially smaller than the EAs of $^{\bullet}NHCH_2CO_2H$ and $^{\bullet}NHPh$, its one-electron reduction potential ($E°$ = +0.04 V) is substantially larger (i.e., more positive or less negative) than those of the latter ($E°$ = −0.38 and −0.23 V, respectively). The larger reduction potential of $^{\bullet}NH_2$ arises because of the particularly favorable $\Delta\Delta G_{solv}$ term (−361.3 kJ mol$^{-1}$), compared with those for the other two systems, which range from −248.9 to −288.2 kJ mol$^{-1}$. This in turn presumably arises because of the smaller size and therefore more concentrated charge in $^{-}NH_2$ compared with the other species.

*3.3.2. EA and E° Values of Heterocyclic Radicals.* The EAs of six nitrogen-containing heterocyclic systems, containing between one and four nitrogen atoms, have been investigated (Figure 3). The computations indicate that the EAs increase roughly linearly as the number of nitrogen atoms is increased

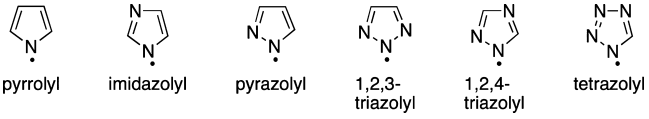


**Figure 3.** Structures of the heterocyclic radicals.

($R^2$ = 0.975). Thus, the EA of pyrrolyl radical (which contains only one nitrogen) is the smallest (208.5 kJ mol$^{-1}$), whereas the EA of the tetrazolyl radical (which contains four nitrogen atoms) is the largest (401.7 kJ mol$^{-1}$). As noted in section 3.1, our calculated EAs for imidazolyl, pyrrolyl, pyrazolyl, and 1,2,3-triazolyl agree well with the experimentally determined values. As far as we are aware, experimentally determined EAs have not yet been reported for the 1,2,4-triazolyl and tetrazolyl radicals.

From a general perspective, the RSEs associated with the radicals become increasingly less positive and even negative as the number of nitrogens is increased. This finding may be rationalized on the basis that, due to the greater electronegativity of N vs C, increasing nitrogen content would tend to render the resulting radicals more electron deficient. In contrast, the ASE values become increasingly positive with increased nitrogen content, and this can be explained, in part, on the basis that the increased electronegativity of N vs C affords a greater degree of stabilization in the anions.

Owing to the large underlying gas-phase EAs, and the favorable $\Delta\Delta G_{solv}$ contributions, all of the heterocyclic radicals are predicted to be oxidizing agents in aqueous solution (i.e., the $E°$ values are positive). The tetrazolyl radical is expected to be a powerful oxidant, with $E°$ = +2.22 V (the largest of any of the nonhalogen radical species considered in this investigation). Of relevance from a biological perspective, the $E°$ of imidazolyl, which serves as a model for the side chain of histidine, is computed to be +0.64 V.

*3.3.3. EA and E° Values of Amidyl Radicals.* We now examine the EAs of a number of amidyl radicals. These species are characterized as having a single electron-withdrawing acyl substituent (i.e., RCO) directly attached to the nitrogen. Such radicals are associated with substantially larger EAs (250.5−384.1 kJ mol$^{-1}$) than typical aminyl-type radicals (e.g., $^{\bullet}NHCH_3$, $^{\bullet}N(CH_3)_2$, $^{\bullet}NHCH_2CO_2H$, and $^{\bullet}NHPh$), which have EAs of 44.5−157.2 kJ mol$^{-1}$. The larger EAs of the amidyl radicals may be attributed to the combination of a destabilizing effect in the radicals (i.e., the RSEs are negative) and a stabilizing effect in the anions (i.e., the ASEs are large and negative).

Destabilizing effects in amidyl radicals have been commented on previously[3a,66] but, in short, arise because it is the unpaired electron, rather than the lone pair, that is better positioned for delocalization into the $\pi^*_{C=O}$ orbital. In this regard, inspection of the Mulliken atomic spin densities (obtained at the B3-LYP/A′VTZ level) for the simplest amide radical ($^{\bullet}NHCHO$) indicate that, although the unpaired electron resides predominantly on the nitrogen atom (0.776 e$^-$), a substantial proportion is also resident on the oxygen atom (0.346 e$^-$). As for stabilizing effects in the amidyl anions, delocalization of the excess negative charge throughout the N−C−O $\pi$-system, allows for a buildup of negative charge on the more electronegative O vs N atom. The atomic polar tensor (APT) charges[67] (obtained at the B3-LYP/A′VTZ level) for $^{-}NHCHO$ indicate the preference for the negative charge to be accommodated on the carbonyl oxygen (charge = −1.068) vs the amido nitrogen (charge = −0.866).

For the more biologically relevant amide radical models, we compute EA values of 250.5 ($^{\bullet}NHCONH_2$), 257.8 ($^{\bullet}N(CH_3)$-CHO), 267.3 ($^{\bullet}NHCOCH_3$), and 280.7 ($^{\bullet}NHCHO$) kJ mol$^{-1}$. It is important to point out that our W1w EAs for $^{\bullet}NHCONH_2$ and $^{\bullet}NHCOCH_3$ differ substantially from those reported on the basis of negative ion mass spectrometry experiments, namely 272.1 and 246.0 kJ mol$^{-1}$, for $^{\bullet}NHCONH_2$ and


dx.doi.org/10.1021/jp310048f | J. Phys. Chem. A 2013, 117, 460−472

Table 3. Comparison of Theoretical and Experimental Appearance Energies (AEs), N−H Bond Dissociation Energies (BDEs), and Electron Affinities (EAs), Relevant to $H_2NCONH_2$ and $H_2NCOCH_3$ (298 K, kJ $mol^{-1}$)

| | AE | | N−H BDE | | EA | |
|---|---|---|---|---|---|---|
| radical | theory[a] | expt[b] | theory[a,c] | expt[b] | theory[a] | expt[b] |
| $^{\bullet}NHCONH_2$ | 207.7 | 183.3 ± 8.7 | 458.2 | 455.4 | 250.5 | 272.1 |
| $^{\bullet}NHCOCH_3$ | 204.8 | 188.1 ± 4.8 | 472.0 | 434.2 | 267.3 | 246.0 |

[a]Calculated at the W1w level. [b]From ref 68. [c]Note that these BDEs are in good agreement with the BDEs from ref 3a calculated at the W2w level: 457.6 ($^{\bullet}NHCONH_2$) and 471.3 ($^{\bullet}NHCOCH_3$) kJ $mol^{-1}$.

$^{\bullet}NHCOCH_3$, respectively.[68] Table 3 compares the experimental appearance energies (AEs) of $^{-}NHCONH_2$ and $^{-}NHCOCH_3$, and N−H bond dissociation energies (BDEs) of $NH_2CONH_2$ and $NH_2COCH_3$, from which the experimental electron affinities (EAs) have been derived (EA = $BDE_{N-H}$ − AE), with the corresponding values obtained at the W1w level. We find that the experimental AE values are lower than our W1w values by 24.4 ($^{\bullet}NHCONH_2$) and 16.7 ($^{\bullet}NHCOCH_3$) kJ $mol^{-1}$. As for the N−H BDEs, although theory and experiment are in close agreement in the case of $H_2NCONH_2$, there is a 37.8 kJ $mol^{-1}$ difference between theory and experiment in the case of $H_2NCOCH_3$. Taken together, the experimentally reported EA for $^{\bullet}NHCONH_2$ is higher than our W1w value by 21.6 kJ $mol^{-1}$, whereas the EA for $^{\bullet}NHCOCH_3$ is lower by 21.3 kJ $mol^{-1}$. This suggests that re-examination of the experimental BDE for $H_2NCOCH_3$ and the AEs for both $^{-}NHCONH_2$ and $^{-}NHCOCH_3$ may be in order.

As expected, the EAs are increased dramatically upon incorporation of either of the electron-withdrawing F or CN substituents in the carbonyl moieties (i.e., as in $^{\bullet}NHCFO$ and $^{\bullet}NHCOCN$), for which we compute EAs of 325.6 and 384.1 kJ $mol^{-1}$, respectively. However, the large difference in EAs between the F- and CN-substituted species (amounting to 58.5 kJ $mol^{-1}$) is striking. On the basis of our analysis, we find that this difference arises almost entirely because of large differences in the extent to which the anions are stabilized (i.e., ASEs of 218.9 and 273.2 kJ $mol^{-1}$, for $^{-}NHCFO$ and $^{-}NHCOCN$, respectively), with only a 4.2 kJ $mol^{-1}$ difference in the RSEs. The large difference between the F- and CN-substituted systems may reflect, in part, the fact that whereas F acts as a $\sigma$-acceptor/$\pi$-donor, CN acts as both a $\sigma$- and $\pi$-acceptor. These two accepting effects would be expected to provide additional stabilization of the anion when the substituent is CN vs F.

We now briefly examine the effect of replacing the C═O moiety with the less-electron-withdrawing C═NH functionality. This modification lowers the EAs of the resulting radicals compared with their carbonyl counterparts. Thus, the EAs of $^{\bullet}NHCH{=}NH$ and $^{\bullet}NH(NH_2)C{=}NH$ are computed to be 198.2 and 204.2 kJ $mol^{-1}$. Given the reduced electron-withdrawing capacity of the imine functional group, the radical species are associated with positive RSE values, compared with the carbonyl derivatives in which the RSEs are negative. On the other hand, the reduced electronegativity of N vs O means that the imine-substituted anions are associated with smaller ASEs (i.e., they are relatively less stabilized) compared with the carbonyl-containing anions.

All of the amidyl radicals considered are associated with positive reduction potentials. Among these, the $^{\bullet}NHCONH_2$ system, which is associated with the smallest gas-phase EA (250.5 kJ $mol^{-1}$), also has the lowest $E^{\circ}$ value (+0.94 V). Furthermore, the $^{\bullet}NHCOCN$ system, which has the largest gas-phase EA (384.1 kJ $mol^{-1}$), has the largest $E^{\circ}$ value in solution (+1.91 V). Finally, consistent with the substantially lower gas-phase EAs of $^{\bullet}NH(H)C{=}NH$ and $^{\bullet}NH(NH_2)C{=}NH$, compared with their amidyl counterparts, the iminyl derivatives are predicted to have low $E^{\circ}$ values (+0.64 and +0.66 V, respectively).

*3.3.4. EA and $E^{\circ}$ Values of Imidyl Radicals.* We now consider the electron affinities of a number of imidyl radicals, which are characterized as having two electron-withdrawing acyl (RCO) groups attached to a central nitrogen atom. Four species of this class have been examined, namely, the parent *N*-formylformamidyl, as well as the cyclic radicals succinimidyl, glutarimidyl, and the biologically important 3-uracilyl (Figure 4).

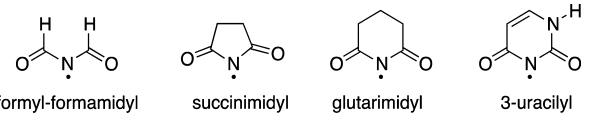


Figure 4. Structures of the imidyl radicals considered in this study.

It is instructive initially to compare the EA of $^{\bullet}N(CHO)_2$ vs $^{\bullet}NHCHO$. We find that, although the EA of the disubstituted system is clearly much larger than the monosubstituted system (390.5 vs 280.7 kJ $mol^{-1}$), the effect on going from one to two formyl substituents is not additive; i.e., a saturation effect exists. In addition, the calculations reveal that the effects of two formyl substituents on the RSE and ASE values of the imide system are also less than additive. Specifically, the RSE of $^{\bullet}N(CHO)_2$ (−52.0 kJ $mol^{-1}$) is slightly less than twice that of $^{\bullet}NHCHO$ (2 × −29.3 = −58.6 kJ $mol^{-1}$), whereas the ASE of $^{-}N(CHO)_2$ (266.4 kJ $mol^{-1}$) is substantially smaller than twice that of $^{-}NHCHO$ (2 × 179.3 = 358.6 kJ $mol^{-1}$).

As for the cyclic imidyl radicals, the ubiquitous succinimidyl system is associated with an EA of 395.9 kJ $mol^{-1}$, whereas glutarimidyl, in which the ring size is increased from five to six, has a substantially smaller EA (350.1 kJ $mol^{-1}$). We find that the smaller EA of glutarimidyl arises via the combined effect of a less negative RSE (by 17.2 kJ $mol^{-1}$) and a less positive ASE (by 28.6 kJ $mol^{-1}$) compared with succinimidyl. Assuming the existence of comparable effects in the parent closed-shell N−H-containing imide parents, the more negative RSE of succinimidyl implies the existence of a larger destabilizing effect compared with glutarimidyl. We note that the Mulliken atomic spin densities (at the B3-LYP/A′VTZ level) for the glutarimidyl and succinimidyl radicals show a greater proportion of the unpaired electron on the more electronegative oxygen atoms in succinimidyl (Figure 5).

Of particular importance to biological systems, we find that the EA of the 3-uracilyl radical is 379.0 kJ $mol^{-1}$. Our value is slightly lower than the EAs obtained previously using more approximate theoretical methods, namely 385.9 kJ $mol^{-1}$ (G2(MP2))[69] and 401.4 kJ $mol^{-1}$ (CBS-Q).[70] In light of the


dx.doi.org/10.1021/jp310048f | J. Phys. Chem. A 2013, 117, 460−472

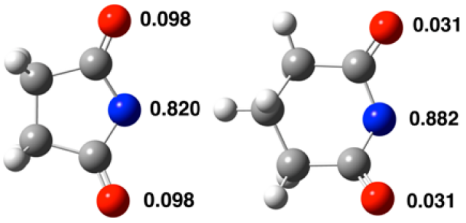


**Figure 5.** Mulliken atomic spin densities obtained at the B3-LYP/A′VTZ level for the succinimidyl and glutarimidyl radicals.

significant discrepancy between the EA of this radical at the W1-F12 and CBS-Q levels (amounting to 22.4 kJ mol$^{-1}$), we attempted to reproduce the CBS-Q value. Our computed CBS-Q EA is 380.8 kJ mol$^{-1}$, which is in good agreement with our W1-F12 result. Additionally, we have also performed calculations using the closely related CBS-QB3 procedure[71] and calculate an EA of 379.9 kJ mol$^{-1}$.

Moving now to the aqueous-phase results, it appears that all of the imidyl radicals are associated with large positive $E°$ values, ranging from +1.79 V (glutarimidyl) to +2.11 V (succinimidyl). The calculated one-electron reduction potential of succinimidyl is in good agreement with the reported experimental value of +2.22 V.[5] Of particular interest from a biological perspective is the finding that the 3-uracilyl radical also has a large positive reduction potential ($E°$ = +2.04 V) and is therefore expected to exhibit strong oxidant behavior. In general, the $E°$ values of the imidyl radicals are substantially larger than those of amidyl radicals, with the notable exception of •NHCOCN, which has an $E°$ value of +1.91 V.

*3.3.5. EA and E° Values of Iminyl Radicals.* The EAs of seven iminyl radicals have been investigated (Table 2). The EAs of these species increase as the electronegativity of the atoms bonded directly to the iminyl moiety increases. Thus, the smallest EA is noted in the case of •N═$CH_2$ (49.1 kJ mol$^{-1}$), whereas the largest occurs for •N═$CF_2$ (258.6 kJ mol$^{-1}$). In aqueous solution, the iminyl radicals are generally predicted to be reducing agents, with $E°$ values typically in the range of −0.76 to −0.31 V. Two exceptions are •N═CH(OH) and •N═$CF_2$ where, by virtue of the larger underlying gas-phase EAs, the $E°$ values are positive. The effect is clearly greater in the case of •N═$CF_2$ ($E°$ = +1.05 V).

**3.4. Preferred Modes of Cleavage of N−X Species (X = Cl and Br).** Comparison of the EA and $E°$ values of Cl• and Br• with the corresponding values for •NRR′ (Table 2) allows for a determination of the thermodynamically preferred mode of cleavage of N−X bonds. In the gas phase, if EA(•NRR′) < EA(•X), then one-electron reduction of the N−X bond would afford •NRR′ and X$^-$, whereas if EA(•NRR′) > EA(•X), formation of X• would be expected. In aqueous solution, if $E°$(•NRR′/$^-$NRR′) < $E°$(•X/X$^-$), then the products of the dissociative one-electron reduction of X−NRR′ are predicted to be •NRR′ and X$^-$. On the other hand, if $E°$(•NRR′/$^-$NRR′) > $E°$(•X/X$^-$), then formation of •X is expected. Before proceeding further, it is of importance to note that our calculated EA and $E°$ values for •Cl and •Br are in good agreement with the experimental values (Table 1). For the EAs, our calculated values of 350.1 and 326.4 kJ mol$^{-1}$ compare well with the experimental values of 348.7 and 324.5 kJ mol$^{-1}$ for •Cl[64i] and •Br,[64j] respectively. For the $E°$ values, our calculated values of +2.39 and +1.80 V compare well with the experimental values[72] of +2.41 and +1.92 V for •Cl and •Br, respectively.

None of the aminyl radicals have EA or $E°$ values that are larger than those of the two halogens, even in the extreme case of substitution by the powerful $\sigma$-electron-withdrawing $CF_3$ group. As a result, one-electron reduction of these species, in either the gas or solution phases, would result in the formation of halide anion plus •NRR′. These observations are consistent with previous experimental findings.[4]

With regards to the heterocyclic species, one-electron reduction of the *N*-bromo derivatives of 1,2,3-triazolyl, 1,2,4-triazolyl, and tetrazolyl would be expected to generate •Br in the gas phase (the EAs being 339.8, 331.1, and 401.7 kJ mol$^{-1}$, compared with 326.4 kJ mol$^{-1}$ for •Br). On the other hand, upon inclusion of solvation corrections, only tetrazolyl has an $E°$ larger than that of •Br (+2.22 vs +1.80 V, respectively), and hence although *N*-bromotetrazole would produce •Br, the other two heterocycles would result in the formation of Br$^-$. Although *N*-chlorotetrazole is predicted to produce •Cl in the gas-phase (EA = 401.7 vs 350.1 kJ mol$^{-1}$, for tetrazolyl and •Cl, respectively), the reverse is true in aqueous solution, with the $E°$ of tetrazolyl (+2.22 V) being smaller than that of •Cl (+2.39 V), thus favoring Cl$^-$ as the product. From a biological perspective, the N-halogenated derivatives formed on the imidazole side-chains of species such as histidine and histamine are thus predicted not to result in halogen atom formation.

The amidyl radicals generally have EA and $E°$ values that are smaller than those of •Cl and •Br. For example, the amidyl radicals considered in this investigation that are most relevant as models for biologically important systems (i.e., •NHCHO, •$NHCOCH_3$, •$NHCONH_2$, and •$N(CH_3)CHO$) have EAs (250.5−280.7 kJ mol$^{-1}$) and $E°$s (+0.94−1.48 V) that are substantially smaller than the values for •Cl and •Br. As a result, N-halogenated amido moieties that might arise as a result of N-halogenation of the peptide linkages in proteins would not be expected to provide a source of halogen atom. It is not until the incorporation of powerful electron-withdrawing substituents, as in •NHCOCN, that halogen atom may be formed. Thus, because the EA of •NHCOCN is 384.1 kJ mol$^{-1}$, which is larger than the EAs of •Cl (350.1 kJ mol$^{-1}$) and •Br (326.4 kJ mol$^{-1}$), one-electron reduction of both ClNHCOCN and BrNHCOCN in the gas phase would be expected to afford the amidyl anion plus either •Cl or •Br, respectively. In aqueous solution, •NHCOCN has a larger $E°$ value than •Br (+1.91 vs +1.80 V) but it has a smaller $E°$ value than •Cl (+2.39 V). As a result, one-electron reduction of BrNHCOCN in water may be expected to provide a source of •Br, but ClNHCOCN would afford Cl$^-$. This switchover for X = Cl on going from the gas to solution phase arises because of the particularly large $\Delta\Delta G_{solv}$ term associated with the •Cl/Cl$^-$ couple, compared with that of •NHCOCN/$^-$NHCOCN (−309.3 vs −239.3 kJ mol$^{-1}$).

For the imidyl species, one-electron reduction of the *N*-chloro and *N*-bromo derivatives of *N*-formylformamide, succinimide, and the biologically relevant 3-uracilyl system would be expected to result in the formation of •Cl or •Br, respectively, in the gas phase. In the case of glutarimide, one-electron reduction of the N-brominated derivative in the gas phase is predicted to afford •Br, but the N-chlorinated derivative would not be expected to significantly favor either glutarimidyl radical or •Cl because the EAs of these two radicals are computed to be virtually equivalent (350.1 kJ mol$^{-1}$). Upon inclusion of solvation corrections, the $E°$ values of •$N(CHO)_2$ (+1.96 V), succinimidyl (+2.11 V), and 3-uracilyl (+2.04 V) are larger than that of •Br (+1.80 V), but smaller than that of •Cl (+2.39 V). As a result, one-electron reduction of the N-


dx.doi.org/10.1021/jp310048f | J. Phys. Chem. A 2013, 117, 460−472

brominated derivatives of these species would be expected to produce •Br, but the N-chlorinated species would produce $Cl^-$. These conclusions are consistent with the experimental findings for *N*-bromosuccinimide and *N*-chlorosuccinimide.[5] Regarding the preferred mode of cleavage of *N*-bromoglutarimide in aqueous solution, the computed $E^\circ$ values of glutarimidyl and •Br are very similar (+1.79 vs +1.80 V, respectively), and as a result a mixture of glutarimidyl radical and •Br is expected. The prediction of a mixture in the case of the cleavage of *N*-bromoglutarimide may explain the relatively more complicated kinetics observed during pulse radiolysis experiments with this system, compared with *N*-bromosuccinimide where the mode of cleavage is more definitive.[5a]

The finding that the *N*-bromo derivative of uracil should give rise to the formation of •Br in aqueous solution is of particular importance from the perspective of disease. First, it is known that the levels of 5-bromouracil are markedly elevated in inflammatory tissue and atherosclerotic lesions in humans,[73] and that the formation of this species may involve formation of the *N*-bromoimide as an intermediate.[2] In addition, levels of uracil are massively elevated in human inflammatory tissue (up to 600 $\mu$M, ca. 1000-fold higher than plasma concentrations).[73] Taken together, these findings suggest that N-brominated derivatives of uracil are likely to be formed with great facility in vivo and, in the presence of reducing agents (such as $O_2^{\bullet-}$, and $Cu^+$ or $Fe^{2+}$), may provide a source of •Br at sites of inflammation.

Finally, none of the iminyl radicals would be expected to give rise to halogen atom formation, in either the gas or solution phases. Of this series of radicals, the largest EA and $E^\circ$ values are noted in the case of •N=$CF_2$ (258.6 kJ $mol^{-1}$ and +1.05 V), which are both well below the corresponding values for •Cl and •Br.

**3.5. Assessment of Lower-Cost Theoretical Procedures for the Calculation of the EAs of •NRR′ Radicals.** In section 3.1, it was demonstrated that the W1w procedure performed well for the calculation of the gas-phase EAs of •NRR′ radicals. On the other hand, application of W1w is currently restricted, because of the limitations of generally available hardware, to the investigation of small to medium-sized species. Therefore, for the benefit of future studies of the EAs of larger systems (which may be of particular importance from a biological perspective), it is necessary to identify appropriate lower-cost theoretical procedures that are usefully reliable. In this final section, a number of standard density functional theory (DFT), double-hybrid DFT (DHDFT), and G*n* theoretical procedures are assessed using as a benchmark the set of 31 gas-phase EAs obtained at the W1w level (Table 2). To ensure an appropriate comparison with the DFT data, secondary effects that are not explicitly included in the DFT calculations, such as relativity and ZPVE corrections, are excluded from the W1w reference values. The resultant all-electron, nonrelativistic, vibrationless W1w reference EAs are given in Table S1 of the Supporting Information.

*3.5.1. Performance of Standard DFT Procedures.* We begin by comparing the performance of a variety of standard DFT procedures (in conjunction with the 6-311+G(3df,2p) basis set) in predicting the EAs of the 31 •NRR′ radicals for which we have obtained W1w data. The mean absolute deviations (MADs), mean deviations (MDs), largest deviations in absolute value (LDs), and the number of systems with a deviation from the benchmark W1w values larger than 10 kJ $mol^{-1}$ (number of outliers, NO) are presented in Table 4.

**Table 4. Performance of DFT Procedures (in Conjunction with the 6-311+G(3df,2p) Basis Set) for the Calculation of Electron Affinities of Nitrogen-Centered Radicals Compared with W1w Reference Values (kJ $mol^{-1}$)**

| functional | type[a] | MAD[b] | MD[b] | LD[b] | NO[b] |
|---|---|---|---|---|---|
| SVWN5 | LDA | 21.9 | +21.7 | 39.8 | 25 |
| B-LYP | GGA | 15.8 | −13.9 | 40.2 | 19 |
| B97-D | GGA | 14.7 | −14.0 | 36.9 | 18 |
| B-P86 | GGA | 10.8 | +3.1 | 21.2 | 17 |
| PBE | GGA | 10.3 | −6.7 | 31.0 | 14 |
| HCTH407 | GGA | 9.4 | +3.5 | 23.6 | 11 |
| M06-L | MGGA | 25.2 | −25.2 | 41.2 | 31 |
| TPSS | MGGA | 20.1 | −20.1 | 40.0 | 26 |
| VSXC | MGGA | 18.8 | −18.6 | 36.1 | 27 |
| $\tau$-HCTH | MGGA | 8.5 | −1.5 | 21.9 | 13 |
| B3-P86 | HGGA | 44.1 | +44.1 | 52.2 | 31 |
| BH&HLYP | HGGA | 38.4 | −38.4 | 52.8 | 31 |
| TPSSh | HGGA | 23.4 | −23.4 | 35.5 | 31 |
| PBE0 | HGGA | 18.3 | −18.3 | 28.2 | 30 |
| B97-1 | HGGA | 16.9 | −14.3 | 32.8 | 29 |
| $\omega$B97X | HGGA | 15.1 | −9.1 | 48.8 | 22 |
| B98 | HGGA | 15.0 | −11.7 | 37.3 | 26 |
| $\omega$B97XD | HGGA | 14.8 | −9.8 | 45.2 | 22 |
| $\omega$B97 | HGGA | 13.0 | −12.9 | 25.2 | 22 |
| B3-PW91 | HGGA | 12.1 | −12.1 | 20.6 | 18 |
| X3-LYP | HGGA | 10.8 | −10.7 | 18.9 | 15 |
| B3-LYP | HGGA | 6.8 | −6.3 | 15.4 | 7 |
| B1-B95 | HMGGA | 20.1 | −20.1 | 28.7 | 31 |
| M06-HF | HMGGA | 18.5 | +18.3 | 36.9 | 22 |
| M05 | HMGGA | 15.5 | −15.5 | 25.8 | 25 |
| BMK | HMGGA | 13.3 | −12.3 | 25.3 | 21 |
| M05-2X | HMGGA | 6.9 | −1.4 | 16.0 | 8 |
| M06 | HMGGA | 5.8 | −5.2 | 13.3 | 4 |
| $\tau$-HCTH-h | HMGGA | 5.4 | −4.5 | 15.5 | 5 |
| M06-2X | HMGGA | 4.8 | −1.4 | 14.8 | 1 |

[a]LDA = local density approximation, GGA = generalized gradient approximation, MGGA = meta-GGA, HGGA = hybrid-GGA, HMGGA = hybrid meta-GGA. [b]MAD = mean absolute deviation, MD = mean deviation, LD = largest deviation, NO = number of outliers (species with absolute deviations of 10 kJ $mol^{-1}$ or larger).

We initially make two general observations. First, 7 of the 31 functionals offer MADs less than 10 kJ $mol^{-1}$, whereas 10 functionals give MADs in the range 10−15 kJ $mol^{-1}$. This finding is consistent with the observation that DFT shows generally reliable performance in the prediction of EAs that correspond to the formation of a closed-shell anion from an open-shell neutral.[74] The generally reliable performance of DFT in such instances has been previously attributed to the fact that the same HOMO is occupied in both the neutral and anionic species, and as a result is well-handled by the Kohn−Sham procedure.[74] Second, most functionals considered in the present study tend to systematically underestimate the EAs (with notable exceptions being SVWN5, B3-P86, and M06-HF).

The LDA functional SVNW5 exhibits relatively poor performance with an MAD of 21.9 kJ $mol^{-1}$, and an LD of 39.8 kJ $mol^{-1}$. Climbing up one rung of Jacob's ladder to the GGA functionals, we note that these exhibit improved performance, with MADs ranging between 9.4 and 15.8 kJ $mol^{-1}$. Regarding the mean deviations of these functionals, whereas B97-D, B-LYP, and PBE have negative MDs


dx.doi.org/10.1021/jp310048f | J. Phys. Chem. A 2013, 117, 460−472

Table 5. Basis-Set Dependence of the Performance of DFT Procedures for the Calculation of the Electron Affinities of Nitrogen-Centered Radicals Compared with W1w Reference Values (MADs, kJ mol$^{-1}$)

| method | type[a] | 6-31+G (d,p) | 6-31+G (2df,p) | 6-311+G (3df,2p) | A′VDZ | A′VTZ | A′VQZ |
|---|---|---|---|---|---|---|---|
| SVWN5 | LDA | 20.4 | 18.2 | 21.9 | 21.7 | 22.8 | 23.2 |
| B-LYP | GGA | 16.5 | 18.1 | 15.8 | 16.1 | 16.3 | 16.6 |
| B97-D | GGA | 14.0 | 16.9 | 14.7 | 14.4 | 15.2 | 15.5 |
| B-P86 | GGA | 9.6 | 10.0 | 10.8 | 11.3 | 11.9 | 12.3 |
| PBE | GGA | 10.1 | 11.8 | 10.3 | 11.0 | 11.4 | 11.8 |
| HCTH407 | GGA | 8.9 | 9.0 | 9.4 | 10.6 | 11.0 | 11.6 |
| M06-L | MGGA | 23.6 | 27.4 | 25.2 | 25.8 | 27.1 | 32.1 |
| TPSS | MGGA | 19.3 | 23.3 | 20.1 | 19.4 | 19.1 | 18.6 |
| VSXC | MGGA | 16.8 | 20.2 | 18.8 | 16.0 | 18.2 | 17.4 |
| $\tau$-HCTH | MGGA | 6.8 | 8.9 | 8.5 | 9.0 | 9.6 | 9.6 |
| B3-P86 | HGGA | 44.7 | 41.2 | 44.1 | 44.8 | 44.4 | 44.3 |
| BH&HLYP | HGGA | 37.2 | 40.6 | 38.4 | 37.1 | 38.0 | 38.1 |
| TPSSh | HGGA | 21.8 | 26.2 | 23.4 | 22.5 | 22.7 | 22.3 |
| PBE0 | HGGA | 17.1 | 20.6 | 18.3 | 17.1 | 17.7 | 17.6 |
| B97-1 | HGGA | 16.6 | 19.0 | 16.9 | 15.6 | 15.9 | 15.7 |
| $\omega$B97-X | HGGA | 14.2 | 16.5 | 15.1 | 13.6 | 15.6 | 15.9 |
| B98 | HGGA | 14.8 | 17.2 | 15.0 | 13.8 | 14.1 | 13.9 |
| $\omega$B97-XD | HGGA | 13.9 | 16.5 | 14.8 | 13.4 | 15.8 | 16.0 |
| $\omega$B97 | HGGA | 12.2 | 14.3 | 13.0 | 11.7 | 14.1 | 14.4 |
| B3-PW91 | HGGA | 11.7 | 14.9 | 12.1 | 11.4 | 11.8 | 11.8 |
| X3-LYP | HGGA | 11.2 | 13.7 | 10.8 | 10.0 | 10.0 | 9.8 |
| B3-LYP | HGGA | 7.6 | 9.5 | 6.8 | 6.5 | 6.4 | 6.5 |
| B1-B95 | HMGGA | 19.1 | 21.9 | 20.1 | 19.0 | 19.7 | 19.6 |
| M06-HF | HMGGA | 19.3 | 13.1 | 18.5 | 12.5 | 24.8 | 30.8 |
| M05 | HMGGA | 13.3 | 15.0 | 15.5 | 11.3 | 21.0 | 20.7 |
| BMK | HMGGA | 15.4 | 16.1 | 13.3 | 14.1 | 12.4 | 14.6 |
| M05-2X | HMGGA | 8.6 | 8.7 | 6.9 | 7.7 | 7.3 | 6.1 |
| M06 | HMGGA | 6.7 | 7.4 | 5.8 | 5.2 | 10.9 | 13.4 |
| $\tau$-HCTH-h | HMGGA | 5.2 | 7.6 | 5.4 | 5.5 | 6.0 | 5.9 |
| M06-2X | HMGGA | 5.3 | 5.9 | 4.8 | 4.9 | 4.6 | 3.6 |

[a]LDA = local density approximation, GGA = generalized gradient approximation, MGGA = meta-GGA, HGGA = hybrid-GGA, HMGGA = hybrid meta-GGA.

(indicating a tendency to underestimate the EAs), HCTH407 and B-P86 are associated with positive MDs.

Of the meta-GGAs, $\tau$-HCTH exhibits the best performance (MAD = 8.5 kJ mol$^{-1}$) and is associated with a low MD (−1.5 kJ mol$^{-1}$), indicating that it is not particularly biased toward overestimation or underestimation of the EAs. The three other meta-GGAs investigated, namely VSXC, TPSS, and M06-L, exhibit poorer performance, with MADs of 18.8, 20.1, and 25.2 kJ mol$^{-1}$, respectively.

The MADs of the hybrid-GGAs span a wide range between 6.8 and 44.1 kJ mol$^{-1}$, with the popular B3-LYP functional being the only functional with an MAD below 10 kJ mol$^{-1}$. Both BH&HLYP and B3-P86 offer very poor performance, with MADs of 38.4 and 44.1 kJ mol$^{-1}$, respectively. The inadequacy of B3-P86 for the prediction of EAs is consistent with previous findings.[74]

The hybrid meta-GGAs M06-2X, $\tau$-HCTHh, M06, and M05-2X show very good performance, with MADs of 4.8, 5.4, 5.8, and 6.9 kJ mol$^{-1}$, respectively. The same four procedures have LDs falling in a narrow range (13.3−16.0 kJ mol$^{-1}$). The worst performing method of this class of functionals is B1-B95, with an MAD of 20.1 kJ mol$^{-1}$, with all radicals having deviations from the W1w values greater than 10 kJ mol$^{-1}$ (i.e., NO = 31).

We now examine the effect of basis set on the performance of the DFT procedures discussed above. To this end, we have considered the performance attained when these functionals are combined with the 6-31+G(d,p), 6-31+G(2df,p) and 6-311+G(3df,2p) Pople-style basis sets, as well as with the A′V$n$Z ($n$ = D, T, Q) correlation-consistent basis sets of Dunning and co-workers (Table 5).

To begin, it appears that 6-311+G(3df,2p) generally provides a comparable performance to that of the A′VQZ basis. In fact, there are some instances in which 6-311+G(3df,2p) performs substantially better than A′VQZ (vide infra). For the most part 6-31+G(d,p) provides comparable performance to 6-311+G-(3df,2p), with MADs generally within 0.0−1.4 kJ mol$^{-1}$ of those obtained with the latter (notable exceptions including SVWN5, BMK, M05-2X, M06, M05, and M06-L for which the deviations are slightly larger at 1.7−2.2 kJ mol$^{-1}$). On the basis of these results, the use of the relatively small 6-31+G(d,p) basis set is expected to be appropriate for the calculation of the EAs of larger systems. For example, the $\tau$-HCTH, B3-LYP, $\tau$-HCTHh, M06-2X and M06 procedures, in conjunction with 6-31+G(d,p) offer MADs of 6.8, 7.6, 5.2, 5.3, and 6.7 kJ mol$^{-1}$, respectively.

The use of the 6-31+G(2df,p) basis set does not appear to warrant its additional cost (compared with 6-31+G(d,p)), as it generally gives rise to larger MADs when used in conjunction with most of the functionals. Thus, the MADs differ by 0.4−2.9 kJ mol$^{-1}$ from those obtained with 6-311+G(3df,2p), compared with 0.0−1.4 kJ mol$^{-1}$ in the case of 6-31+G(d,p).

For some functionals, such as M06-HF, M05, and M06, the use of the A′VTZ or A′VQZ basis sets instead of A′VDZ leads to a notable deterioration in performance. For example, M06 gives rise to the following MADs: 5.2 (A′VDZ), 10.9 (A′VTZ) and 13.4 (A′VQZ) kJ mol$^{-1}$.

*3.5.2. Double-Hybrid Density Functional Theory Procedures.* We now examine the performance of the double-hybrid density functional theory (DHDFT) procedures (Table 6). These calculations have been carried out with the A′V*n*Z (*n* = D, T, Q) basis sets.

**Table 6. Statistical Analysis of the Performance of Double-Hybrid Density Functional Theory Procedures for the Calculation of the Electron Affinities of •NRR′ Radicals Compared with W1w Values (kJ mol$^{-1}$)**

| functional | basis set[a] | MAD | MD | LD | NO |
|---|---|---|---|---|---|
| B2K-PLYP | A′VDZ | 7.5 | −5.1 | 18.4 | 11 |
| B2GP-PLYP | A′VDZ | 7.0 | −5.8 | 14.7 | 8 |
| B2-PLYP | A′VDZ | 6.8 | −6.5 | 13.6 | 6 |
| ROB2-PLYP | A′VDZ | 6.0 | −5.9 | 12.7 | 4 |
| DuT | TZ[b] | 6.6 | +6.4 | 28.6 | 6 |
| PoT | TZ[c] | 5.4 | +1.3 | 24.7 | 3 |
| B2K-PLYP | A′VTZ | 5.8 | 0.0 | 25.0 | 3 |
| B2GP-PLYP | A′VTZ | 4.4 | −1.4 | 15.5 | 2 |
| B2-PLYP | A′VTZ | 3.8 | −3.1 | 10.4 | 1 |
| ROB2-PLYP | A′VTZ | 3.1 | −2.4 | 7.8 | 0 |
| B2K-PLYP | A′VQZ | 5.6 | +2.3 | 28.6 | 3 |
| B2GP-PLYP | A′VQZ | 4.0 | +0.7 | 18.7 | 3 |
| B2-PLYP | A′VQZ | 3.0 | −1.5 | 9.3 | 0 |
| ROB2-PLYP | A′VQZ | 2.5 | −0.9 | 6.5 | 0 |

[a]A′V*n*Z denotes the use of aug′-cc-pV*n*Z basis sets (*n* = D, T, Q). [b]The DuT procedure uses the cc-pVTZ basis set on H and the aug-cc-pVTZ basis set with a set of tight d functions on all other elements (see ref 50). [c]The PoT procedure uses the 6-311+G(3df,2p) basis set with a set of tight *d* functions on all elements (see ref 50).

The performance improves on going from B2K-PLYP ⇒ B2GP-PLYP ⇒ B2-PLYP ⇒ ROB2-PLYP. Furthermore, the basis set convergence follows the expected pattern, improving from A′VDZ ⇒ A′VTZ ⇒ A′VQZ. In conjunction with the A′VQZ basis set, ROB2-PLYP offers the best performance, with an MAD of 2.5 kJ mol$^{-1}$ and a small LD of just 6.5 kJ mol$^{-1}$. The next best performer is B2-PLYP (MAD = 3.0 kJ mol$^{-1}$), whereas B2K-PLYP, which was parametrized for thermochemical kinetics, gives an MAD of 5.6 kJ mol$^{-1}$. The use of the A′VTZ basis set in conjunction with any of the four procedures does not come with a significant loss in accuracy. Thus, the increase in the MAD of the ROB2-PLYP procedure in conjunction with the A′VTZ vs A′VQZ basis set amounts to only 0.6 kJ mol$^{-1}$, with a corresponding increase in the LD of just 1.3 kJ mol$^{-1}$.

The recently reported DuT and PoT procedures,[50] which were parametrized for use with Dunning-type and Pople-type basis sets of triple-ζ-quality, do not offer improved performance for the present systems compared with that of the other DHDFTs when they are used with the A′VTZ basis set. The PoT procedure is marginally better than DuT, with MADs of 5.4 and 6.6 kJ mol$^{-1}$, respectively. The DuT procedure tends to systematically overestimate the EAs, with an MD of +6.4 kJ mol$^{-1}$ and had six outliers associated with deviations larger than 10 kJ mol$^{-1}$. The PoT procedure offers performance similar to that of B2K-PLYP, but not as good as that of the other procedures in conjunction with the A′VTZ basis set.

*3.5.3. Performance of Gn-Type Procedures.* Table 7 presents the statistical analysis of the performance of a selection of composite procedures of the G*n* family relative to the W1w benchmark values.[75] The calculations were carried out with the B3-LYP/A′VTZ geometries that are used to obtain the W1w reference energies, and not the B3-LYP/6-31G(2df,p) geometries prescribed for most of these procedures.

**Table 7. Statistical Analysis of the Performance of G*n* Methods for the Calculation of the Electron Affinities of •NRR′ Radicals Compared with W1w Values (kJ mol$^{-1}$)**

| method | MAD | MD | LD | NO |
|---|---|---|---|---|
| G4(MP2) | 5.2 | 0.0 | 17.8 | 5 |
| G4(MP2)-6X | 4.2 | +1.4 | 13.6 | 3 |
| G3X(MP2) | 4.2 | +2.5 | 14.6 | 1 |
| G4-5H | 3.1 | +2.3 | 8.2 | 0 |
| G3X(MP2)-RAD | 3.0 | +2.9 | 6.6 | 0 |
| G4(MP2)-6X+ | 2.7 | +1.5 | 8.1 | 0 |
| G4 | 2.6 | −0.8 | 11.2 | 2 |
| G3X | 2.4 | −1.2 | 11.7 | 1 |

The best-performing methods are G3X, G4, and G4(MP2)-6X+, with MADs of 2.4, 2.6, and 2.7 kJ mol$^{-1}$, respectively. G4(MP2)-6X+ is an attractive choice because it is substantially more economical in terms of time and computational resources than G3X or G4. The G3X(MP2)-RAD procedure also offers good performance (MAD = 3.0 kJ mol$^{-1}$) and is associated with the smallest LD of all the G*n* procedures (6.6 kJ mol$^{-1}$). The use of the restricted-open-shell (RO) formalism leads to a substantial improvement compared with the unrestricted-based G3X(MP2) procedure, which has an MAD 1.2 kJ mol$^{-1}$ larger than its RO-counterpart. Furthermore, the LD of G3X(MP2) is more than twice that of G3X(MP2)-RAD (14.6 vs 6.6 kJ mol$^{-1}$). The two procedures exhibit comparable MDs (+2.5 and +2.9 kJ mol$^{-1}$), with a tendency to slightly overestimate the EAs.

The worst performing of the G*n* procedures is G4(MP2), with an MAD of 5.2 kJ mol$^{-1}$. The inclusion of additional scaling parameters, as in the G4(MP2)-6X procedure, results in improved performance (MAD = 4.2 kJ mol$^{-1}$). Additionally, improving the underlying CCSD(T) calculation through the use of a basis set that includes sp- and d-diffuse functions, as in the G4(MP2)-6X+ procedure, substantially improves the performance (MAD = 2.7 kJ mol$^{-1}$). Similar observations have been made for the EA subset of the G2/97 set.[58]

## 4. CONCLUDING REMARKS

Through a high-level (W1w) quantum chemical investigation of the gas-phase electron affinities (EAs) and aqueous-phase one-electron reduction potentials ($E°$) of the radicals arising from homolytic cleavage of X−NRR′ bonds (namely •NRR′ and X• where X = Cl and Br), insights have been gained regarding the preferred mode of cleavage of these species upon one-electron reduction.

(1) Depending on the substituents attached to the nitrogen, the EAs of nitrogen-centered radicals span a wide range (357.2 kJ mol$^{-1}$). For example, whereas the EA of •$NHCH_3$ is 44.5 kJ mol$^{-1}$, the EAs of the succinimidyl and tetrazolyl radicals are computed to be 395.9 and 401.7 kJ mol$^{-1}$, respectively. Likewise, the aqueous one-electron reduction potentials ($E°$)


dx.doi.org/10.1021/jp310048f | J. Phys. Chem. A 2013, 117, 460−472

vary from −0.90 V ($^{\bullet}N(CH_3)_2$) to +2.11 and +2.22 V for succinimidyl and tetrazolyl, respectively.

(2) From a biological perspective, the EA and $E^{\circ}$ values of aminyl radicals (e.g., $^{\bullet}NHCH_2CO_2H$ and $^{\bullet}NHPh$), heterocyclic species such as pyrrole and imidazole, and relevant amidyl radicals (e.g., $^{\bullet}NHCHO$, $^{\bullet}NHCOCH_3$, $^{\bullet}N(CH_3)CHO$, $^{\bullet}NHCONH_2$) that are not substituted with powerful electron-withdrawing substituents (such as F and CN), are all significantly smaller than those of $Cl^{\bullet}$ and $Br^{\bullet}$. As a result, the N-chlorinated or N-brominated precursors are predicted to cleave in such a way as to generate a nitrogen-centered radical plus a halide anion.

(3) In the gas phase, one-electron reductions of the N-chlorinated and N-brominated derivatives of the imides (i.e., *N*-formylformamide, succinimide, glutarimide, and uracil) are predicted to give rise to halogen atom formation. In aqueous solution on the other hand, the N-brominated derivatives are predicted to produce $Br^{\bullet}$, whereas the N-chlorinated derivatives would afford $Cl^{-}$.

(4) The finding that one-electron reduction of *N*-bromouracil should provide a source of $Br^{\bullet}$ has important implications in terms of inflammatory-related diseases. For example, $Br^{\bullet}$ is known to participate in hydrogen-atom abstractions from the $\alpha$-C−H moieties of amino acids (leading to protein degradation). Furthermore, reaction of $Br^{\bullet}$ with excess $Br^{-}$ affords $Br_2^{\bullet-}$, a potent oxidant capable of oxidizing nucleobases in plasmid DNA. These processes may be expected to further potentiate host damage upon repeated inflammatory events.

To facilitate future studies of the gas-phase EAs of larger $^{\bullet}NRR'$ radicals, the performance of a range of lower-cost theoretical procedures has been evaluated against a test set of 31 EAs obtained at the W1w level. The methods examined include standard density functional theory (DFT) and double-hybrid DFT (DHDFT) procedures, as well a number of composite G*n* thermochemical protocols. A number of important points have emerged.

(1) Approximately half of the standard DFT procedures offer MADs of ≤15.0 kJ mol$^{-1}$, even when used in conjunction with relatively small basis sets. The following standard DFT procedures afford relatively accurate gas-phase EAs using the small 6-31+G(d,p) basis set, with MADs of 5.2 ($\tau$-HCTHh), 5.3 (M06-2X), 6.7 (M06), 6.8 ($\tau$-HCTH), and 7.6 (B3-LYP) kJ mol$^{-1}$. The corresponding MADs in conjunction with the much larger 6-311+G(3df,2p) basis set are 4.8 (M06-2X), 5.4 ($\tau$-HCTHh), 5.8 (M06), 6.8 (B3-LYP), and 8.5 ($\tau$-HCTH) kJ mol$^{-1}$.

(2) Of the double-hybrid DFT procedures, ROB2-PLYP and B2-PLYP offer the best performance, with MADs of 2.5 and 3.0 kJ mol$^{-1}$, respectively (in conjunction with the A′VQZ basis set). They also perform well with the smaller A′VTZ basis set (with MADs of 3.1 and 3.8 kJ mol$^{-1}$, respectively).

(3) Of the composite G*n* procedures, G3X, G4, and G4(MP2)-6X+ offer the best performance, with MADs of 2.4, 2.6, and 2.7 kJ mol$^{-1}$, respectively. However, G4(MP2)-6X + has the advantage of a significantly reduced computational cost.

## ■ ASSOCIATED CONTENT

### Supporting Information

W1w electronic energies, ZPVEs, thermal corrections to enthalpies and entropies, and free energy of solvation corrections necessary to compute the EA and $E^{\circ}$ values for all species, as well as %TAE$_e$[(T)] diagnostics (Table S1); B3-LYP/A′VTZ geometries (Cartesian coordinates) (Table S2); and full citations for references 59−61 (Table S3). This material is available free of charge via the Internet at http://pubs.acs.org.

## ■ AUTHOR INFORMATION

### Corresponding Author

*E-mail: L.R., radom@chem.usyd.edu.au; R.J.O., robert.oreilly@utas.edu.au.

### Notes

The authors declare no competing financial interest.

## ■ ACKNOWLEDGMENTS

We gratefully acknowledge funding (to A.K. and L.R.) from the Australian Research Council, and the generous allocation of computing time from the National Computational Infrastructure (NCI) National Facility and from Intersect Australia Ltd. We thank Professor Michael Davies and Dr. David Pattison (Heart Research Institute) for helpful discussions.

## ■ REFERENCES

(1) (a) Malle, E.; Marsche, G.; Arnhold, J.; Davies, M. J. *Biochim. Biophys. Acta* **2006**, *1761*, 392−415. (b) Davies, M. J.; Dean, R. T. *Radical-Mediated Protein Oxidation: From Chemistry to Medicine*; Oxford University Press: Oxford; New York, 1997.

(2) Pattison, D. I.; Davies, M. J. *Curr. Med. Chem.* **2006**, *13*, 3271−3290 and references therein..

(3) (a) O'Reilly, R. J.; Karton, A.; Radom, L. *J. Phys Chem A* **2011**, *115*, 5496−5504. (b) O'Reilly, R. J.; Karton, A.; Radom, L. *Int. J. Quantum Chem.* **2012**, *112*, 1862−1878.

(4) (a) Hawkins, C. L.; Davies, M. J. *Biochem. J.* **1998**, *332*, 617−625. (b) Hawkins, C. L.; Davies, M. J. *Biochem. J.* **1999**, *340*, 539−548. (c) Hawkins, C. L.; Davies, M. J. *J. Chem. Soc., Perkin Trans. 2* **1998**, 1937−1946. (d) Hawkins, C. L.; Rees, M. D.; Davies, M. J. *FEBS Lett.* **2002**, *510*, 41−44.

(5) (a) Pattison, D. I.; O'Reilly, R. J.; Skaff, O.; Radom, L.; Anderson, R. F.; Davies, M. J. *Chem. Res. Toxicol.* **2011**, *24*, 371−382. (b) Lind, J.; Shen, X.; Eriksen, T. E.; Merenyi, G.; Eberson, L. *J. Am. Chem. Soc.* **1991**, *113*, 4629−4633.

(6) Easton, C. J. *Chem. Rev.* **1997**, *97*, 53−82.

(7) Wardman, P. *J. Phys. Chem. Ref. Data* **1989**, *18*, 1637−1756.

(8) Candeias, L. P.; Steenker, S. *J. Am. Chem. Soc.* **1989**, *111*, 1094−1099.

(9) Milligan, J. R.; Aguilera, J. A.; Nguyen, T.-T. D.; Ward, J. F.; Know, Y. W.; He, B.; Cunningham, R. P. *Radiat. Res.* **1999**, *151*, 334−342.

(10) (a) Martin, J. M. L.; Oliveira, G. *J. Chem. Phys.* **1999**, *111*, 1843−1856. (b) Parthiban, S.; Oliveira, G.; Martin, J. M. L. *J. Phys. Chem. A* **2001**, *105*, 895−904. (c) Parthiban, S.; Martin, J. M. L. *J. Chem. Phys.* **2001**, *114*, 6014−6029. (d) Oren, M.; Iron, M. A.; Burcat, A.; Martin, J. M. L. *J. Phys. Chem. A* **2004**, *108*, 7752−7761. (e) Karton, A.; Rabinovich, E.; Martin, J. M. L.; Ruscic, B. *J. Chem. Phys.* **2006**, *125*, 144108 (1−16). (f) Karton, A.; Daon, S.; Martin, J. M. L. *Chem. Phys. Lett.* **2011**, *510*, 165−178.

(11) (a) Dunning, T. H. *J. Chem. Phys.* **1989**, *90*, 1007−1023. (b) Kendall, R. A.; Dunning, T. H.; Harrison, R. J. *J. Chem. Phys.* **1992**, *96*, 6796−9806. (c) Dunning, T. H., Jr.; Peterson, K. A.; Wilson, A. K. *J. Chem. Phys.* **2001**, *114*, 9244−9253.

(12) Merrick, J. P.; Moran, D.; Radom, L. *J. Phys. Chem. A* **2007**, *111*, 11683−11700.

(13) (a) Douglas, M.; Kroll, N. M. *Ann. Phys.* **1974**, *82*, 89. (b) Heß, B. A. *Phys. Rev. A* **1986**, *33*, 3742−3748.

(14) Curtiss, L. A.; McGrath, M. P.; Blaudeau, J.-P.; Davis, N. E.; Binning, R.; Radom, L. *J. Chem. Phys.* **1995**, *103*, 6104−6113.

(15) (a) Barone, V.; Cossi, M. *J. Phys. Chem. A* **1998**, *102*, 1995−2001. (b) Cossi, M.; Rega, N.; Scalmani, G.; Barone, V. *J. Comput. Chem.* **2003**, *24*, 669−681.
(16) Takano, Y.; Houk, K. N. *J. Chem. Theory Comput.* **2005**, *1*, 70−77.
(17) Reiss, H.; Heller, A. *J. Phys. Chem.* **1985**, *89*, 4207−4213.
(18) Perdew, J. P.; Ruzsinszky, A.; Tao, J.; Staroverov, V. N.; Scuseria, G. E.; Csonka, G. I. *J. Chem. Phys.* **2005**, *123*, 062201 (1−9).
(19) Vosko, S. H.; Wilk, L.; Nusair, M. *Can. J. Phys.* **1980**, *58*, 1200−1211.
(20) Becke, A. D. *Phys. Rev. A* **1988**, *38*, 3098−3100.
(21) Lee, C.; Yang, W.; Parr, R. G. *Phys. Rev. B* **1988**, *37*, 785−789.
(22) Perdew, J. P. *Phys. Rev. B* **1986**, *33*, 8822−8824.
(23) (a) Perdew, J. P.; Burke, K.; Ernzerhof, M. *Phys. Rev. Lett.* **1996**, *77*, 3865−3868. (b) Erratum: *Phys. Rev. Lett.* **1997**, *78*, 1396.
(24) Boese, A. D.; Handy, N. C. *J. Chem. Phys.* **2001**, *114*, 5497−5503.
(25) Grimme, S. *J. Comput. Chem.* **2006**, *27*, 1787−1799.
(26) van Voorhis, T.; Scuseria, G. E. *J. Chem. Phys.* **1998**, *109*, 400−410.
(27) Tao, J. M.; Perdew, J. P.; Staroverov, V. N.; Scuseria, G. E. *Phys. Rev. Lett.* **2003**, *91*, 146401 (1−4).
(28) Boese, A. D.; Handy, N. C. *J. Chem. Phys.* **2002**, *116*, 9559−9569.
(29) Zhao, Y.; Truhlar, D. G. *J. Chem. Phys.* **2006**, *125*, 194101 (1−18).
(30) Adamo, C.; Barone, V. *J. Chem. Phys.* **1999**, *110*, 6158−6170.
(31) Becke, A. D. *J. Chem. Phys.* **1993**, *98*, 5648−5652.
(32) Perdew, J. P.; Chevary, J. A.; Vosko, S. H.; Jackson, K. A.; Pederson, M. R.; Singh, D. J.; Fiolhais, C. *Phys. Rev. B* **1992**, *46*, 6671−6687.
(33) Hamprecht, F. A.; Cohen, A. J.; Tozer, D. J.; Handy, N. C. *J. Chem. Phys.* **1998**, *109*, 6264−6271.
(34) Schmider, H. L.; Becke, A. D. *J. Chem. Phys.* **1998**, *108*, 9624−9631.
(35) Staroverov, V. N.; Scuseria, G. E.; Tao, J.; Perdew, J. P. *J. Chem. Phys.* **2003**, *119*, 12129−12137.
(36) Stephens, P. J.; Devlin, F. J.; Chabalowski, C. F.; Frisch, M. J. *J. Phys. Chem.* **1994**, *98*, 11623−11627.
(37) Xu, X.; Zhang, Q.; Muller, R. P.; Goddard, W. A., III. *J. Chem. Phys.* **2005**, *122* (014105), 1−14.
(38) Becke, A. D. *J. Chem. Phys.* **1993**, *98*, 1372−1377.
(39) Chai, J.-D.; Head-Gordon, M. *J. Chem. Phys.* **2008**, *128*, 084106 (1−15).
(40) Chai, J.-D.; Head-Gordon, M. *Phys. Chem. Chem. Phys.* **2008**, *10*, 6615−6620.
(41) Becke, A. D. *J. Chem. Phys.* **1996**, *104*, 1040−1046.
(42) Boese, A. D.; Martin, J. M. L. *J. Chem. Phys.* **2004**, *121*, 3405−3416.
(43) Zhao, Y.; Schultz, N. E.; Truhlar, D. G. *J. Chem. Phys.* **2005**, *123*, 161103 (1−4).
(44) Zhao, Y.; Schultz, N. E.; Truhlar, D. G. *J. Chem. Theory Comput.* **2006**, *2*, 364−382.
(45) Zhao, Y.; Truhlar, D. G. *Theor. Chem. Acc.* **2008**, *120*, 215−241.
(46) Grimme, S. *J. Chem. Phys.* **2006**, *124*, 034108 (1−16).
(47) Tarnopolsky, A.; Karton, A.; Sertchook, R.; Vuzman, D.; Martin, J. M. L. *J. Phys. Chem. A* **2008**, *112*, 3−8.
(48) Karton, A.; Tarnopolsky, A.; Lamere, J.-F.; Schatz, G. C.; Martin, J. M. L. *J. Phys. Chem. A* **2008**, *112*, 12868−12886.
(49) Graham, D. C.; Menon, A. S.; Goerigk, L.; Grimme, S.; Radom, L. *J. Phys. Chem. A* **2009**, *113*, 9861−9873.
(50) Chan, B.; Radom, L. *J. Chem. Theory Comput.* **2011**, *7*, 2852−2863.
(51) Curtiss, L. A.; Redfern, P. C.; Raghavachari, K.; Pople, J. A. *J. Chem. Phys.* **2001**, *114*, 108−117.
(52) Curtiss, L. A.; Redfern, P. C.; Raghavachari, K. *J. Chem. Phys.* **2007**, *127*, 124105 (1−8).
(53) Henry, D. J.; Sullivan, M. B.; Radom, L. *J. Chem. Phys.* **2003**, *118*, 4849−4860.
(54) Curtiss, L. A.; Redfern, P. C.; Raghavachari, K. *J. Chem. Phys.* **2007**, *126*, 084108 (1−12).
(55) Chan, B.; Coote, M. L.; Radom, L. *J. Chem. Theory Comput.* **2010**, *6*, 2647−2653.
(56) Curtiss, L. A.; Redfern, P. C.; Raghavachari, K. *J. Chem. Phys.* **2007**, *127*, 124105 (1−8).
(57) Chan, B.; Deng, J.; Radom, L. *J. Chem. Theory Comput.* **2011**, *7*, 112−120.
(58) Karton, A.; O'Reilly, R. J.; Chan, B.; Radom, L. *J. Chem. Theory Comput.* **2012**, *8*, 3128−3136.
(59) Frisch, M. J.; Trucks, G. W.; Schlegel, H. B.; Scuseria, G. E.; Robb, M. A.; Cheeseman, J. R.; Scalmani, G.; Barone, V.; Mennucci, B.; Petersson, G. A.; et al. *Gaussian 09*, Revision A.1 ; Gaussian Inc.; Wallingford, CT, 2009 (full citation given in the Supporting Information).
(60) Frisch, M. J.; Trucks, G. W.; Schlegel, H. B.; Scuseria, G. E.; Robb, M. A.; Cheeseman, J. R.; Montgomery, Jr., J. A.; Vreven, T.; Kudin, K. N.; Burant, J. C.; et al. *Gaussian 03*, Revision E.1; Gaussian Inc.; Wallingford, CT, 2004 (full citation given in the Supporting Information).
(61) Werner, H.-J.; Knowles, P. J.; Lindh, R.; Manby, F. R.; Schütz, M.; Celani, P.; Korona, T.; Mitrushenkov, A.; Rauhut, G.; B. Adler, T.; et al. *MOLPRO* 2009.1; see http://www.molpro.net (full citation given in the Supporting Information).
(62) Curtiss, L. A.; Raghavachari, K.; Trucks, G. W.; Pople, J. A. *J. Chem. Phys.* **1991**, *94*, 7221−7230.
(63) (a) Curtiss, L. A.; Raghavachari, K.; Redfern, P. C.; Pople, J. A. *J. Chem. Phys.* **1997**, *106*, 1063−1079. (b) Curtiss, L. A; Redfern, P. C; Raghavachari, K.; Pople, J. A *Chem. Phys. Lett.* **2002**, *109*, 42−55.
(64) (a) Wickham-Jones, C. T.; Ervin, K. M.; Ellison, G. B.; Lineberger, W. C. *J. Chem. Phys.* **1989**, *91*, 2762−2763. (b) Radisic, D.; Xu, S.; Bowen, K. H., Jr. *Chem. Phys. Lett.* **2002**, *354*, 9−13. (c) Drzaic, P. S.; Brauman, J. I. *J. Phys. Chem.* **1984**, *8*, 5285−5290. (d) Gianola, A. J.; Ichino, T.; Hoenigman, R. L.; Kato, S.; Bierbaum, V. M.; Lineberger, W. C. *J. Phys. Chem. A* **2005**, *109*, 11504−11514. (e) Gianola, A. J.; Ichino, T.; Hoenigman, R. L.; Kato, S.; Bierbaum, V. M.; Lineberger, W. C. *J. Phys. Chem. A* **2004**, *108*, 10326−10335. (f) Gianola, A. J.; Ichino, T.; Kato, S.; Bierbaum, V. M.; Lineberger, W. C. *J. Phys. Chem. A* **2006**, *110*, 8457−8466. (g) Ichino, T.; Andrews, D. H.; Rathbone, G. J.; Misaizu, R.; Caliva, R. M. D.; Wren, S. W.; Kato, S.; Bierbaum, V. M.; Lineberger, W. C. *J. Phys. Chem. B* **2008**, *112*, 545−557. (h) Cowles, D. C.; Travers, M. J.; Frueh, J. L.; Ellison, G. B. *J. Chem. Phys.* **1991**, *94*, 3517−3528. (i) Martin, J. D. D.; Hepburn, J. W. *J. Chem. Phys.* **1998**, *109*, 8139−8142. (j) Blondel, C.; Cacciani, P.; Delsart, C.; Trainham, R. *Phys. Rev. A* **1989**, *40*, 3698−3701.
(65) Karton, A.; Martin, J. M. L. *J. Chem. Phys.* **2012**, *136*, 124114 (1−12).
(66) Wood, G. P. F.; Henry, D. J.; Radom, L. *J. Phys. Chem. A* **2003**, *107*, 7985−7990.
(67) (a) Cioslowski, J. *J. Am. Chem. Soc.* **1989**, *111*, 8333−8336. (b) De Proft, F.; Martin, J. M. L; Geerlings, P. *Chem. Phys. Lett.* **1996**, *250*, 393−401.
(68) Muftakhov, M. V.; Vasil'ev, Y. V.; Mazunov, V. A. *Rapid Commun. Mass Spectrom.* **1999**, *13*, 1104−1108.
(69) Hanel, G.; Gstir, B.; Denifl, S.; Scheier, P.; Probst, M.; Farizon, B.; Farizon, M.; Illenberger, E.; Mark, T. D. *Phys. Rev. Lett.* **2003**, *90*, 188104 (1−4).
(70) Li, X.; Sanche, L.; Sevilla, M. D. *J. Phys. Chem. B* **2004**, *108*, 5472−5476.
(71) Montgomery, J. A.; Frisch, M. J.; Ochterski, J. W.; Petersson, G. A. *J. Chem. Phys.* **1999**, *110*, 2822−2827.
(72) Lind, J.; Jonsson, M.; Eriksen, T. E.; Merenyi, G.; Eberson, L. *J. Phys. Chem.* **1993**, *97*, 1610−1614.
(73) Henderson, J. P.; Byun, J.; Takeshita, J.; Heinecke, J. W. *J. Biol. Chem.* **2003**, *278*, 23522−23528.
(74) Rienstra-Kiracofe, J. C.; Tschumper, G. S.; Schaefer, H. F., III. *Chem. Rev.* **2002**, *102*, 231−282.
(75) We have also evaluated the performance of the G*n* procedures relative to the experimental values reported in Table 1. We find that

they are associated with the following MADs (in kJ $mol^{-1}$): G4 (4.1), G3X (5.0), G4(MP2) (5.4), G4(MP2)-6X+ (5.6), G4-5H (5.6), G3X(MP2)-RAD (6.2), and G4(MP2)-6X (6.3). In comparison, the W1w procedure, our primary benchmark in this investigation, achieves an MAD from experimental values of 2.9 kJ $mol^{-1}$.